ARCHIVES OF ACOUSTICS
14, 1-2, 11-27 (1989)

AN EXPERIMENTAL LITHOTRIPSY SYSTEM FOR THE STUDY OF SHOCK WAVE EFFECTS

LESZEK FILIPCZYŃSKI, JERZY ETIENNE, ANNA GRABOWSKA, TOMASZ WASZCZUK

Institute of Fundamental Technological Research, Polish Academy of Sciences
(00–049 Warszawa, ul. Świętokrzyska 21)

HENRYK KOWALSKI

Department of Biophysics Medical Academy, Warsaw, Chałubińskiego 5

MICHAŁ GRYZIŃSKI, JACEK STANISŁAWSKI

Institute of Nuclear Problems, Świerk

The authors have developed a lithotripsy system and measurement set-up for the study of shock wave interaction with living tissues. The system consists of an electromagnetical shock wave generator, focusing lens and capacitance pressure pulse measuring hydrophones. The shock wave pulse pressures obtained with this system can be changed up to 40 MPa (about 400 atm). An additional ultrasonic system enables measurements of the gas bubbles generation, an important factor in the destruction process caused by cavitation. Details of the system concerning the shock wave generation, pressure field distribution, pressure time dependence and measurement technique as well as its practical application possibilities are discussed in the paper.

Autorzy opracowali system litotrypsera i układy pomiarowe dla badań oddziaływania fal uderzeniowych z żywymi tkankami. System złożony jest z elektromagnetycznego generatora fal uderzeniowych, ogniskującej soczewki i hydrofonów pojemnościowych umożliwiających bezwzględne pomiary impulsów ciśnienia.

Ciśnienia uzyskiwane za pomocą opracowanego systemu mogą osiągać wartości aż do 40 MPa (około 400 atm.). Dodatkowy układ ultradźwiękowy pozwala na pomiary generacji pęcherzyków powietrza, które są istotnym czynnikiem w procesie niszczenia tkanek powodowanym przez kawitację. Szczegóły systemu generacji fal uderzeniowych, rozkładów pól ciśnienia, zależności ciśnienia od czasu, technika pomiarowa oraz praktyczne możliwości zastosowania systemu przedyskutowano w artykule.

Introduction

Lithotripsy is becoming nowadays an important therapeutical means in the work of many urological clinical centers. However, as it is a relatively new method, mechanisms of shock wave interaction with living tissues are far from being known. Many important practical problems have to be solved, especially those connected with the dosage of this powerful technique. For the study of these problems the authors have developed a lithotripsy system and a pressure pulse measurement method.

1. The shock wave generator

The elaborated system consists of an Eisenmenger (electromagnetic) shock generator [8] with a focusing lens [18]. Figure 1 presents the idea of the system. The condenser C is charged through the rectifier D to a voltage which can be changed

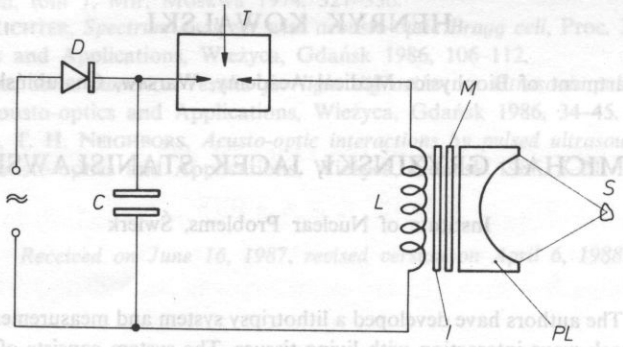

FIG. 1. The idea of the experimental lithotrypsy system

from $U_0 = 17$ to 25 kV. Then it is discharged through a plane coil L with a repetition rate about 1 Hz. The coil is coupled through an isolating plastic foil I with the metal membrane M. The high amplitude current pulse generates eddy currents in the membrane. In this way a strong magnetic field is induced which causes a force pressing the membrane in the opposite direction to the coil L. The membrane M is coupled acoustically with a plastic focusing lens PL. In this way a plane wave generated by the membrane is focused at the kidney stone S.

Figure 2 presents the shape of the high voltage pulse U and the shape of the current pulse I. The frequency of the oscillations equals 98 kHz and the current amplitude is equal to 10 kA.

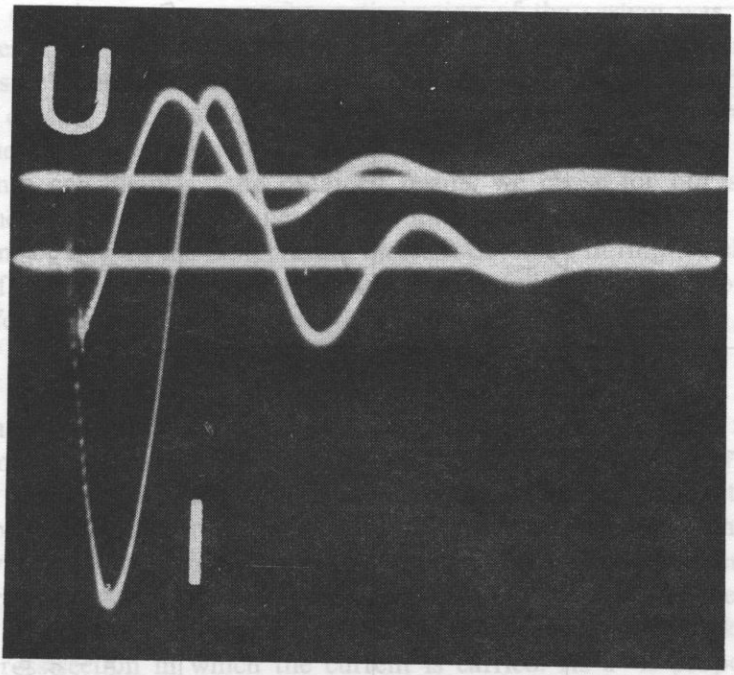

FIG. 2. Shapes of the high voltage U and current I flowing in the coil

The diameter of the plane coil equals 140 mm. To obtain a high electric coupling with the metal membrane, the coil was composed of four parallel windings of the copper wire 0.6 mm in diameter. The number of turns was equal to 4×27. The diameter of the wire was chosen taking into consideration the skin effect. The depth of the skin effect layer [20]

$$\varepsilon^E = \frac{1}{2\pi}\sqrt{\frac{\varrho^E \cdot 10^9}{\mu f}}\,[\mathrm{cm}] \underset{\mathrm{Cu},20^\circ\mathrm{C}}{=} 6.62/\sqrt{f}\ \ [\mathrm{cm}] \tag{1}$$

equals 0.2 mm for copper when $f = 100$ kHz, ϱ^E denotes here the resistivity in Ω cm, f – frequency in Hz, $\mu = 1$ is permeability for copper and aluminium.

In this way, using four instead of one winding, it was possible to decrease the distance between the current carried by the wire cross-section and the metal membrane.

The distance between the coil and the membrane, depending on the thickness of the insulating foil, was the next factor limiting the electrical coupling between the coil and the membrane. Polycarbonate foil Makrofil N (Beyer AG) was used as insulating material. Figure 3 shows the acoustic pressure in the form of our system as the function of the thickness of the insulating foil. For reasons of electric strength we chose a foil thickness ranging from 0.3 to 0.4 mm.

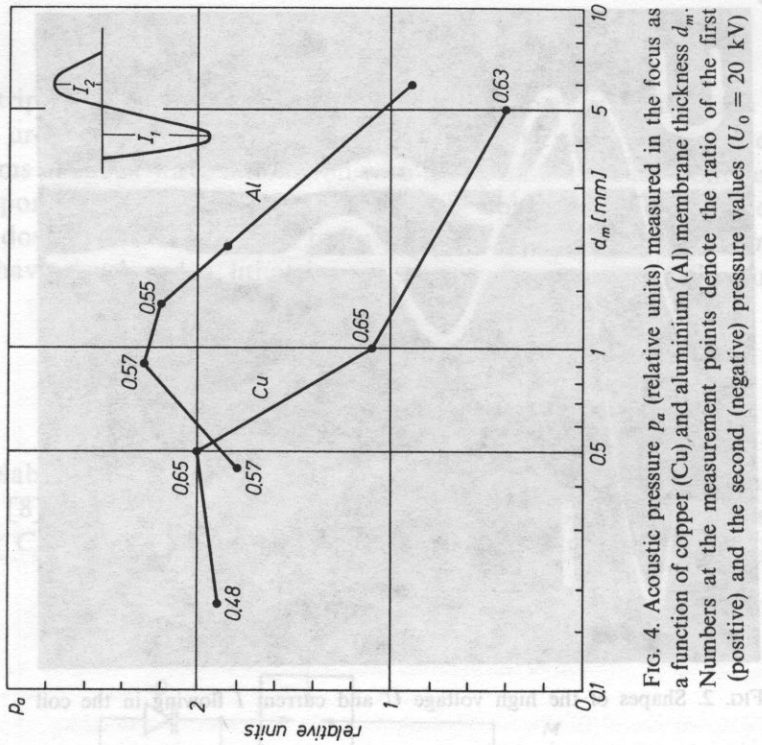

FIG. 4. Acoustic pressure p_a (relative units) measured in the focus as a function of copper (Cu) and aluminium (Al) membrane thickness d_m. Numbers at the measurement points denote the ratio of the first (positive) and the second (negative) pressure values ($U_0 = 20$ kV)

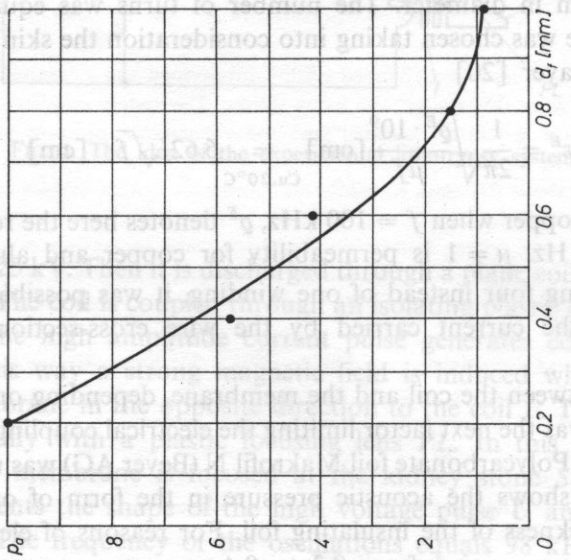

FIG. 3. Acoustic pressure p_a (relative units) measured in the focus as a function of the insulating foil thickenss d_f ($U_0 = 20$ kV)

The next experiment necessary for optimization of the system was performed with two types of membranes made of copper and aluminium. Figure 4 presents the acoustic pressure obtained in the focus as the function of the membrane thickness. It is difficult to explain this result depending on electrical and acoustical properties of the membranes as well as on electrical and acoustical conditions in which they work.

Taking into consideration the obtained results we chose for our system the aluminium membrane with a thickness of 1.35 mm. Aluminium shows an advantage from the point of view of the temperature increase observed during the shock wave generation. If the membrane diameter is constant, the following expression seems to be decisive for temperature changes:

$$CP = (c_w \varrho d)(\lambda d)/\sqrt{\varrho^E}, \tag{2}$$

where c_w denotes specific heat, d optimum thickness of the membrane, ϱ its density, λ coefficient of thermal conductivity. The product in the first brackets is proportional to the heat necessary to increase of the membrane, the product in the second brackets is proportional to the heat flowing toward a cooling brass ring, coupled mechanically with the membrane at its circumference. The last term in the denominator corresponds to electrical losses which depend on the electrical resistivity ϱ^E and on the skin depth ε^E. The value of ε^E determines the thickness of the membrane cross-section in which the current is carried. As ε^E is proportional to $\sqrt{\varrho^E}$ (see Eq. (1)), one obtains in the result the form given in Eq. (2).

The higher the value of CP, the lower the temperature increase during the shock wave generation. Inserting into Eq. (2) the corresponding coefficients [13] and optimum values of aluminium and copper membrane thickness, one obtain the ratio $CP_{AL}/CP_{Cu} \approx 3$. It shows that the increase of temperature will be smaller in the case of the aluminium membrane. Equation (2) is approximative as it does not take into account the influence of the membrane electrical resistance on the generated pressure value. However, Fig. 4 shows that the maximum measured pressure difference for copper and aluminium membranes is not higher than 15%.

2. The pressure field

The wave produced by the metal membrane becomes distorted as it travels throught the medium. In some distance called critical distance [2] the slope of the pulse front becomes infinite, i.e., a discontinuity appears in the wave. The critical distance for a plane wave equals [17]

$$x = \sigma/\beta\varepsilon k \tag{3}$$

where $\beta = 1 + B/2A$, B/A – ratio of nonlinearity parameters (for water $B/A = 5.4$ [2], for various soft tissues $B/A = 5.5$–11 [7]), c_0 – wave velocity for small amplitudes, $\varepsilon = u_0/c_0$ – acoustical Mach number, $u_0 = p/\varrho c_0$ – particle velocity at

the wave source, p – wave pressure, σ – shock parameter, $k = 2\pi f/c_0$, f – frequency of the wave.

One should take into account the fact that the wave frequency is in our case two times greater than the frequency of the electric current in the coil shown in Fig. 1. This is caused by the square dependence of the generated pressure p, on the current I carried by the coil [8]

$$p \doteq I^2. \tag{4}$$

This was confirmed by measurements of the half period time $T/2 = 2.6$ μs near the pressure source (see Fig. 7) which corresponds to the frequency of 198 kHz.

Equation (3) can be transformed to the following expression used sometimes in the literature:

$$x = c_0\sigma\left[(1+B/2A)\frac{p}{\varrho c_0}\frac{1}{c_0}2\pi f\right]^{-1} = \varrho c_0^3\sigma T[\pi(2+B/A)p]^{-1} = \varrho c_0^3\sigma[\pi(2+B/A)pf]^{-1}. \tag{5}$$

In the case of a focused wave, generated by a concave transducer, the critical is shifted by the distance [17]

$$\Delta X = Z_0\exp(-x/z_0) \tag{6}$$

toward the transducer, z_0 denotes its focal length.

The focus should be situated near the critical distance to obtain the maximum slope and, simultaneously, the maximum amplitude of the pressure pulse. According to the paper [1], for shock parameters $1.6 > \sigma \geqslant 1$ one does not observe any significant decrease of the pulse amplitude and the front slope.

Assuming the pressure in focus equal to $p' = 20$ MPa and the gain (in linear approximation) of the lens [19]

$$\frac{p'}{p} = \frac{kr^2}{2z_0} = 10, \tag{7}$$

where $k = 2\pi f/c_0$, one obtains for shock parameters $\sigma = 1.6$ and 1, for focal length $z_0 = 20$ cm, radius of the lens $r = 7$ cm, frequency $f = 198$ kHz, from Eqs. (5) and (6) the shift of the focus relatively to the critical distance. It is equal to $x = 1$ cm and 3 cm, respectively. These values seem to be acceptable since the – 6 dB drop of the pressure along the lens axis occurs in the distance of 4 cm before the focus (see Fig. 7).

To estimate the influence of the focusing lens on the pressure distribution and on its maximum value, we applied the linear theory and the continuous wave

approximation, neglecting the attenuation and internal reflections in our 1 cm thick perspex lens. However, we took into account transmission depending on acoustical parameters of the two media and on the incident angle of the acoustical rays. The transmission coefficient was determined from Eq. [14]:

$$D_{l/l} = \frac{2}{N} \frac{\varrho_W c_W \cos\alpha_L \cos 2\alpha_T}{\varrho_L c_L \cos\alpha_W}, \tag{8}$$

where

$$N = \left(\frac{c_T}{c_L}\right)^2 \sin\alpha_L \sin 2\alpha_T + \cos^2 2\alpha_T + \frac{\varrho_W c_W}{\varrho_L c_L} \frac{\cos\alpha_L}{\cos\alpha_W} \tag{9}$$

ϱ_L, ϱ_W denote, respectively, the density of lens and water, c_L, c_T – velocity of longitudinal and transverse waves in lens, c_W – wave velocity in water, α_L – incident angle of longitudinal wave, α_T – reflection angle of the transverse wave in lens, α_W refraction angle of the wave in water.

The calculated values of D as the function incident angle α_L is shown in Fig. 5.

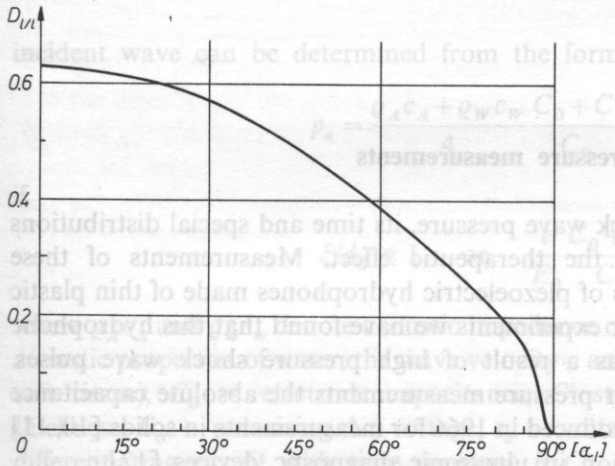

FIG. 5. Transmission coefficient $D_{L/l}$ on the concave boundary perspex water of the lens. α_L – incident angle of the longitudinal wave

Basing on the paper [19], the axial distribution of the pressure could be computed for the spherical lens taking into account the transmission loss on this concave boundary. The maximum pressure and the focal length depend strongly on the frequency as shown in Fig. 6. Hence one can conclude that the sharper the shock wave pulse, the higher the gain of the lens.

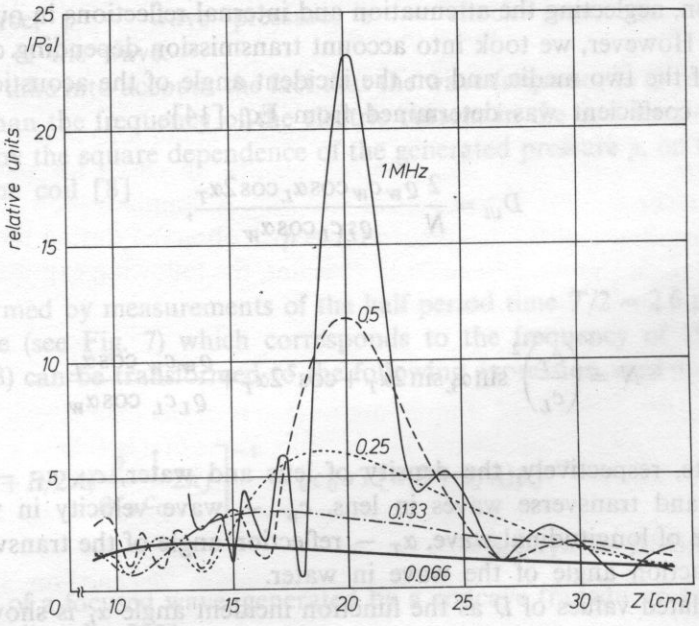

FIG. 6. Pressure distribution along the lens axis computed for various frequencies of the continuous wave. p — axial pressure in relation to the pressure on the plane lens surface (linear approximation)

3. Pressure measurements

The value of the acoustic shock wave pressure, its time and special distributions are very important factors for the therapeutic effect. Measurements of these parameters are possible by means of piezoelectric hydrophones made of thin plastic layer PVDF. However during our experiments we have found that this hydrophone was distroyed in a short time as a result of high pressure shock wave pulses. Therefore we decided to adapt for pressure measurements the absolute capacitance transducer method which was introduced in 1966 for measurements in solids [10, 11] and then for dosage determination in ultrasonic diagnostic devices [12].

The idea of this hydrophone is shown in Fig. 7. The ultrasonic pulse P penetrates the boundary water-metal plate and then it is totally reflected from the second boundary between the metal plate and air. Vibrations of this boundary change the capacitance C_0 which is formed by the second metal boundary and the electrode. The electrode is polarized with the d.c. voltage E_0 through a high value resistance R. In this way the electric charge in the capacitance C_0 remains constant while its value changes due to boundary vibrations. Hence the electric voltage on the capacitance C_0 changes, too, giving the output signal e. It is easy to show that the pressure of the

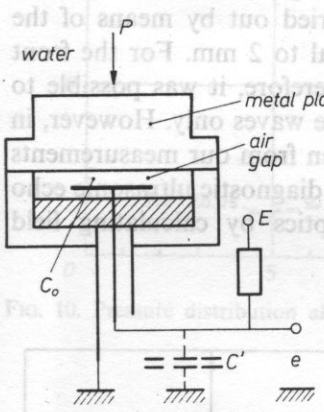

FIG. 7. Capacitance hydrophone

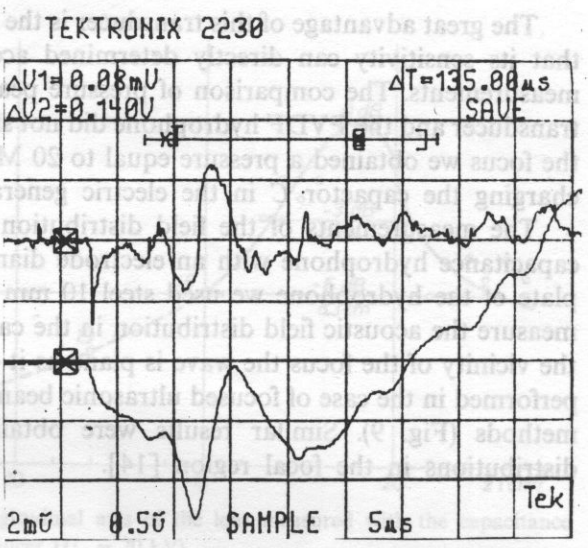

FIG. 8. Particle velocity $u \div de/dt$ (uper curve) and displacement $\xi \div e$ lower curve measured by means of the capacitance transducer (reversed polarization)

incident wave can be determined from the formula

$$p_a = \frac{\varrho_A c_A + \varrho_W c_W}{4} \frac{C_0 + C'}{C_0} \frac{d_0}{E_0} \frac{e_d}{R_d C_d} \tag{10}$$

if

$$\xi/d_0 \ll 1 \quad \text{or} \quad \frac{e}{E_0} \frac{C_0 + C'}{C_0} \ll 1, \tag{11a, b}$$

where $\varrho_A c_A$ and $\varrho_w c_w$ denote acoustic impedance of the metal plate and of water (the acoustic properties of water, the wave velocity c and density ϱ are almost the same as soft tissue), C_0 – electrode capacitance, C' stray capacitances, d_0 – air gap thickness, E_0 – polarizing d.c. voltage, e_d – voltage on the output of an additional differentiating circuit with time constant $R_d C_d$, ξ – displacement.

Figure 8 presents a typical result of measurements with the capacitance hydrophone recorded on the plotter. The lower curve is the signal e on the transducer output before differentiation. It is proportional to the displacement of ξ the medium particles. Important are the first 2 microseconds after the initial pulse. Later one obtains many internal reflections inside the transducer which form a complicated pattern due to interferences. The upper curve shows the same signal after diffraction. It represents the velocity u of the medium particles and after multiplication by the parameters shown in Eq. 7 it is equal to this pressure.

The great advantage of this transducer is the linearity of its metal [9] and the fact that its sensitivity can directly determined according to Eq. (11) from electrical measurements. The comparison of pressure peak values obtained by means of this transducer and the PVDF hydrophone did not show a difference greater than 3%. In the focus we obtained a pressure equal to 20 MPa for the d.c. voltage U_0 of 20 kV charging the capactor C in the electric generator (see Fig. 1).

The measurements of the field distribution were carried out by means of the capacitance hydrophone with an electrode diameter equal to 2 mm. For the front plate of the hydrophone we used steel 10 mm thick. Therefore, it was possible to measure the acoustic field distribution in the case of plane waves only. However, in the vicinity of the focus the wave is plane as it can be seen from our measurements performed in the case of focused ultrasonic beams used in diagnostic ultrasonic echo methods (Fig. 9). Similar results were obtained in optics by calculating field distributions in the focal region [14].

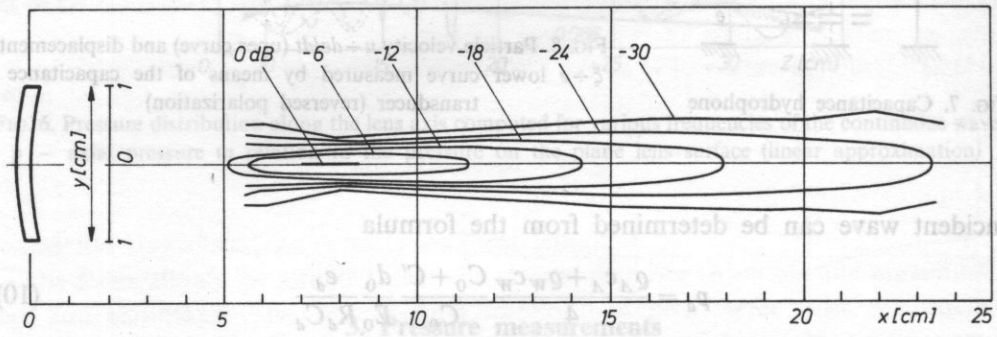

FIG. 9. Iso-echo-amplitude curves of the ultrasonic beam radiated by the ultrasonograph UG-4. The y axis is 2 times englarged when compared with the x-axis. Frequency 2.5 MHz, transducer radius 1 cm [12]

The results of our measurement of the pressure distribution along the lens axis are shown in Fig. 10. Outside of the focus, where the wave is no more plane, the measurement results may not correspond to the true pressure values. For instance, in the distance of 5 cm for the electrode radius of 1 mm the external acoustic ray, coming from the lens, will be shifted by 0.25 mm passing the aluminium plate. This may cause an error which decreases with the distance. Therefore the dotted line in Fig. 10 representing the pressure distribution measured along the longitudinal axis is an approximative one. The length of the focus measured on the $-$ 6 dB level is equal to 8.3 cm.

The numbers at the measurement points denote the duration time of the first half period of the propagation pulse. At the distance of 5 cm it was equal to 2.6 μs corresponding to the frequency of 198 kHz. With the distance the pulse became

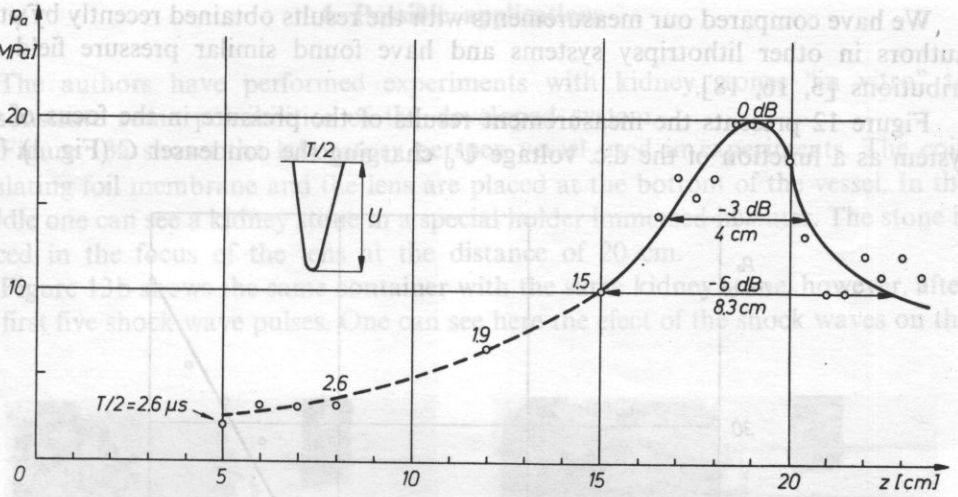

FIG. 10. Pressure distribution along the longitudinal axis of the lens measured with the capacitance transducer ($U_0 = 20$ kV)

distorted and we measured in this case the duration time between the first zero crossing points. In the focus it was equal to 0.3 μs and the rise time – 50 ns. However, in fact the rise time may be shorter since this was the sampling period of the digital oscilloscope used in measurements.

Figure 11 presents the measured pressure distribution in the focus perpendicularly to the direction of the shock wave propagation. The focus in this direction is about 10 times shorter than in the longitudinal one. Its width measured on the – 6 dB equals 8.5 mm.

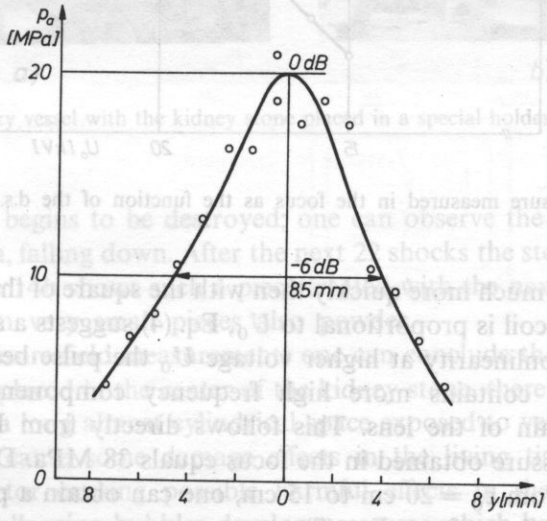

FIG. 11. Pressure distribution in the focal plane ($U_0 = 20$ kV)

We have compared our measurements with the results obtained recently by other authors in other lithotripsy systems and have found similar pressure field distributions [3, 16, 18].

Figure 12 presents the measurement results of the pressure in the focus of our system as a function of the d.c. voltage U_0 charging the condenser C (Fig. 1). The

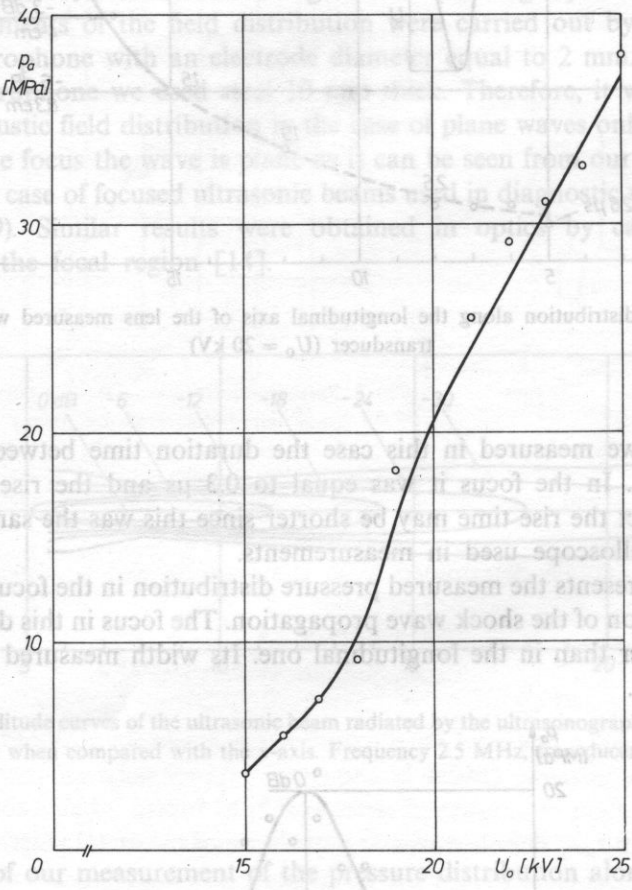

FIG. 12. Pressure measured in the focus as the function of the d.s. voltage U_0

pressure p increases much more quickly then with the square of the voltage U_0. Since the current I in the coil is proportional to U_0, Eq. (4) suggests a square dependence. However, due to nonlinearity at higher voltage U_0 the pulse becomes sharper and then the spectrum contains more high frequency components thus increasing considerably the gain of the lens. This follows directly from Fig. 6.

The highest pressure obtained in the focus equals 38 MPa. Decreasing the focal length of the lens from $z_0 = 20$ cm to 15 cm, one can obtain a pressure increase of about 10% as it follows from Eq. (7).

4. Possible applications

The authors have performed experiments with kidney stones "in vitro" to demonstrate some possibilities of the developed system.

Figure 13a shows the laboratory perspex vessel used in experiments. The coil, insulating foil membrane and the lens are placed at the bottom of the vessel. In the middle one can see a kidney stone in a special holder immersed in water. The stone is placed in the focus of the lens at the distance of 20 cm.

Figure 13b shows the same container with the same kidney stone, however, after the first five shock wave pulses. One can see here the efect of the shock waves on the

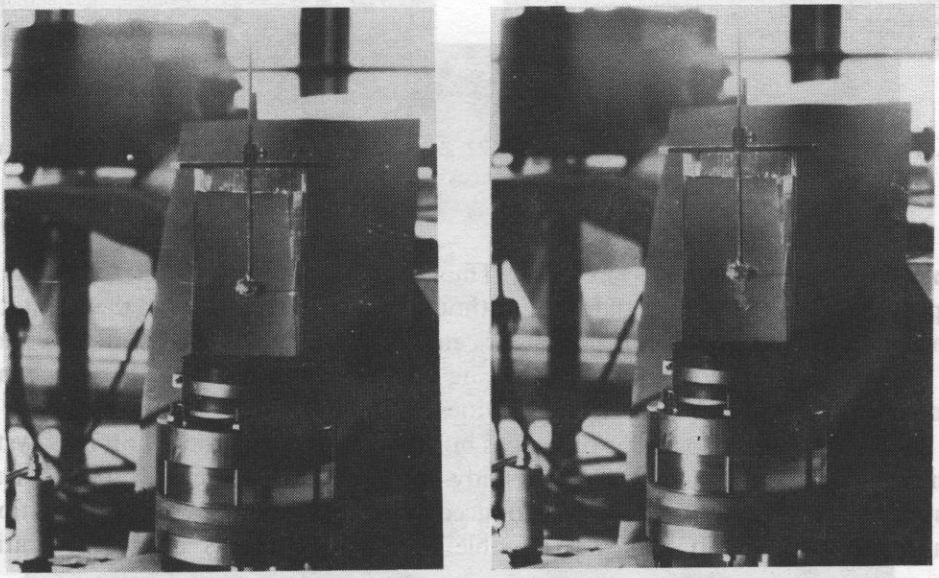

FIG. 13. The laboratory vessel with the kidney stone placed in a special holder (a) and after 5 shocks (b)

stone. The stone begins to be destroyed; one can observe the powder of the stone, caused by erosion, falling down. After the next 22 shocks the stone breaks into pieces (Fig. 14a). Figure 14b shows such a piece treated with the next 25 shocks. One can notice apart from very small pieces also powder.

From the pressure field measurements one can conclude that even if the focus of the lithotripsy is placed in the center of the kidney stone, there will be in the kidney, before the stone, a long almost cylindrical space exposed to very high pressures (see Fig. 10). It may cause some damage effects in the living tissues.

The main factor causing possible harmful effects in the tissue seems to be cavitation. The collapsing bubbles develop pressures which have been measured to

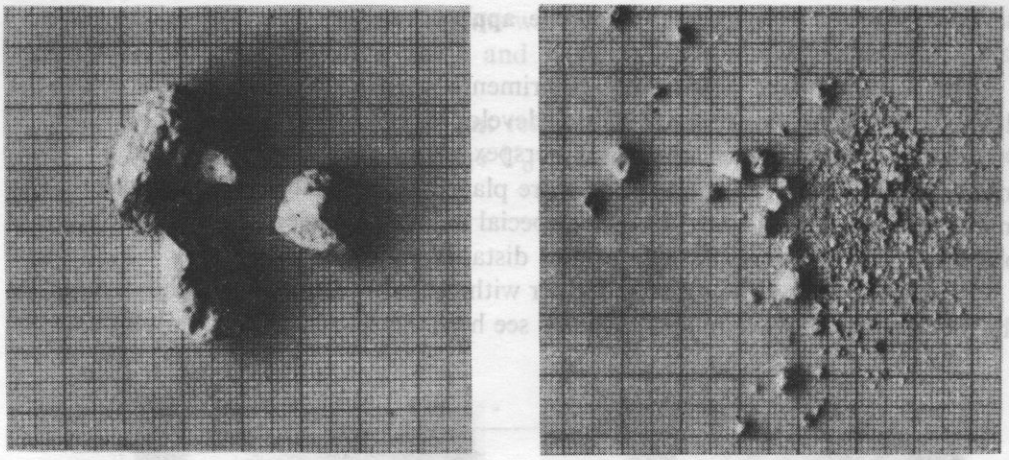

FIG. 14. The disintegrated stone after the next 22 shocks (a), one piece of the stone after the next 25 shocks (b)

achieve values as high as 300 MPa. Thus cavitation must be considered as an important factor in tissue damage. Although the total energy of the cavitation process is small, the concentration of this energy into a very small volume results in an enormous energy density, producing such very high pressures and high temperatures within the collapsing cavities [4].

In this situation knowledge of the gas bubble generation in the lithotrypsy system seems to be very important for the study of the possible damage process in soft tissues. For this purpose we have introduced into the described system an additional echoscope (Fig. 15). It makes it possible to observe the gas bubble generation,

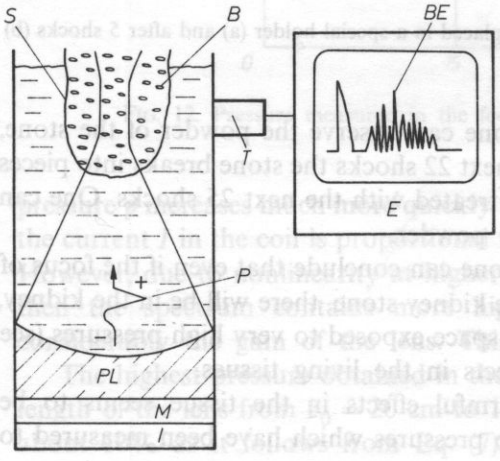

FIG. 15. The system for the gas bubble study. S – tested space, S – tested space with gas bubbles or with biological specimen, B – gas bubble, BE – bubble echoes, T – transducer, E – echoscope, P – pressure pulse, PL – plastic lens, M – membrane, I – insulating sheet

measurements of their life time to observe their growth and collapse under the action of shock wave pulses and to determine their density and size, if possible. Figure 16 presents as an example an echogram of gas bubbles were generated in water by the shock wave pulse of 20 MPa pressure.

There is of course the question whether cavitation can exist "in vivo" in the case of very short stress pulses and if it can produce damage to the living tissue. Recently, it has been demonstrated that the shock wave pulses used in lithotripsy can really produce "in vivo" acoustic cavitation in the blood vessels of pigs [5]. Also haemorrhages in all kidney structures in dogs could be shown [6]. Thus changes were dose-dependent.

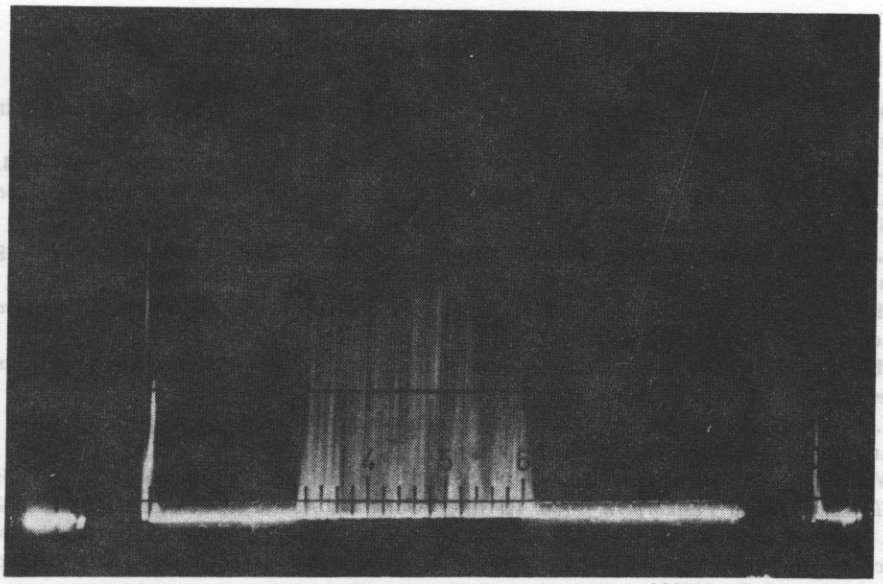

FIG. 16. Echogram of gas bubbles generated by the shock wave pulse of 20 MPa pressure. Transducer frequency — 3 MHz

In this situation one can conclude that it is important and necessary to study all the biological effects which are caused by high pressure shock wave pulses in tissues. Only by collecting many experimental data from this type of research can one elaborate dosage rules. It is necessary to answer the question what is the highest permitted pressure value, its duration time, its shape, positive and negative components, repetition period, therapy time and other factors to eliminate or to decrease the possible harmful effects in the patients treated with this powerful new therapy technique.

5. Conclusions

The developed system can be used for the study of biological effects caused by shock waves at high pressures. The values of pressures and their spatial distributions and time dependence correspond with those used in lithotripsy. This could be confirmed experimentally by destroying several kidney stones "in vitro" too. Thus the described system after some adaptations can be used as the main part of a lithotripter for clinical applications.

The applied capacitance hydrophones were verified experimentally in shock wave measurements at very high pulse pressure levels with no sign of any serious damage.

References

[1] D. BACON, *Finite amplitude distortion of the fields used in diagnostic ultrasound*, Ultrasound in Med. and Biol., **10**, 1, 189–195 (1984).

[2] R. T. BAYER, *Nonlinear acoustics*, U.S. Naval Sea Systems Command. Washington 1974.

[3] A. COLEMAN et al., *Pressure waveforms generated by a Dornier extra corporal shock-wave lithotrypter*. Ultrasound in Med and Biol, **13**, 561–657 (1987).

[4] L. A. CRUM, Cavitation microprojects as a contributory mechanisms for renal calculi desintegration in ESWL. Journal of Urology (1988) [in print].

[5] M. DELIUS, I. EIZENHOFER, R. DENK, H. LEIBICH, W. BRENDEL, *Biological effects of shock waves*, J. Acoust. Soc. Am., Suplement S XX (1988).

[6] M. DELIUS et al, *Biological effects of shock waves: Kidney damage by shock waves in dogs. Dose dependence*. Ultrasound in Med. and Biol. **14**, 117–122 (1988).

[7] F. DUNN, W. K. LAW, L. A. FRIZELL, *The ultrasonic nonlinearity parameter for biological media*, Archives of Acoustics, **9**, 1–2, 29–34 (1984).

[8] W. EISENMENGER, *Eine elektromagnetische Impulsschallquelle zur Erzeugung von Druckstössen in Flussigkeiten und Festkorpern*. Proc. III Inter. Cong. on Acoustics, Stuttgart 326–329 (1959).

[9] J. ETIENNE, L. FILIPCZYŃSKI, A. GRABOWSKA, T. WASZCZUK, *Pressure measurements in nonlinear acoustics by means of capacitance and PVDF hydrophones*, Proc. XXXV Open Seminar Acoustics, Białowieża, Poland 1988.

[10] L. FILIPCZYŃSKI, *Measuring pulse intensity of ultrasonic longitudinal and transverse waves in solids*, Proc. Vibration Problems, **7**, 1, 31–46 (1966).

[11] L. FILIPCZYŃSKI, *Absolute measurements of particle velocity displacement or intensity of ultrasonic pulses in liquids and solids*, Acoustics, **21**, 173–180 (1969).

[12] L. FILIPCZYŃSKI, G. ŁYPACEWICZ, J. SAŁKOWSKI, *Intensity determination of the inside of the abdomen by means of ultrasonics*, Proc. Vibration Problems, **7**, 3, 211–220 (1966).

[13] R. GRIMSEHL, R. TOMASCHEK, *Lehrbuch der Physik*, Bd. I p. 590, 658, Bd. II p. 197, 198.

[14] J. H. KRAUTKRÄHER, *Werkstoffprufung mit Ultrasschall*, Springer-Berlin 1961, p. 473 also Ultrasonic Testing Materials, Springer, Berlin 1983 p. 607.

[15] E. LINFOOT, E. WOLF, *Phase distribution near focus in an abberation free diffraction image*. Proc. Phys. Soc. B, **69**, 823–832 (1956).

[16] J. MESTAS, *Generation et focalization d'une onde de choc en vue de la destruction transparentale des calculs*, Int. National des Sciences Appliques. Lyon Doctor Thesis 1982.

[17] T. MUIR, L. CARSTENSEN, *Prediction of nonlinear acoustic effects at biomedical frequencies and intensities*, Ultrasound in Med. and Biol. **6**, 4, 345–357 (1980).

[18] H. REICHENBERG, G. NASER, *Electromagnetic acoustic source for the extracorporal generation of shock waves in lithotrypsy*, Siemens Forschung und Entwielungs Berichte **15**, 187–194 (1986).
[19] U. SCHLENGERMANN, *Schallfeldausbildungs bei ebenen Ultraschallquellen mit fokusierenden Linsen*, Acoustics, **30**, 6, 291–300 (1974).
[20] F. E. TERMAN, *Radio Engineers Handbook*, McGraw Hill, New York 1943, p. 34.

Received on 8 November, 1988.